

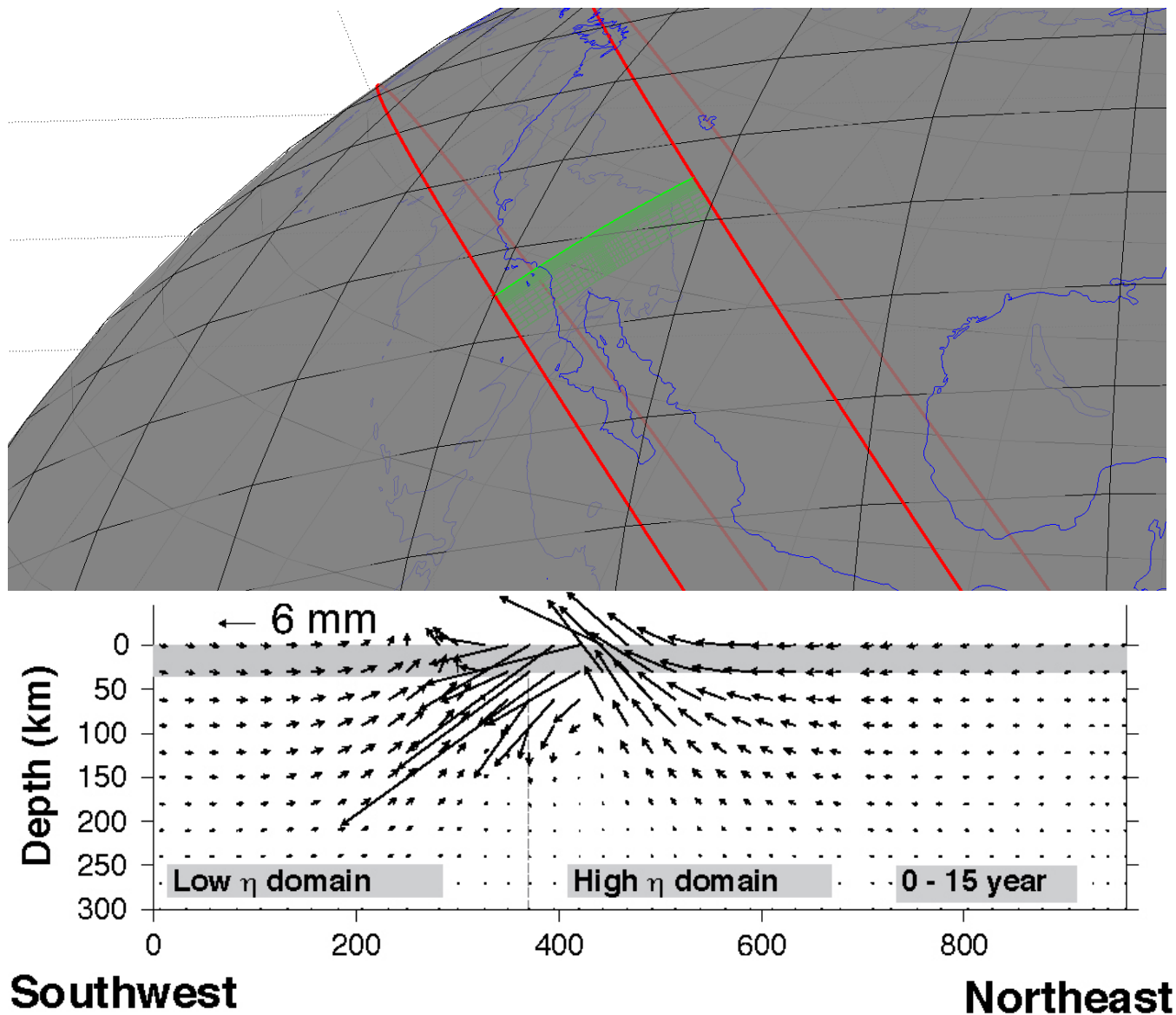
VISCO2.5D

Version 1.0 Tutorial

Fred F. Pollitz

2015 CIDER Workshop
UC Berkeley

July 13, 2015 (code and tutorial last edited 08/11/2022)



Acknowledgements

I thank Bill Broadley and Laurent Montesi for helping get this software ready for distribution at the 2015 CIDER Workshop.

Christina Morency and Brad Aagaard provided useful comments on the manuscript that led to the development of this software. I am grateful to Andrew Bradley for invaluable assistance with the implementation of the linear algebra package.

I thank Kaj Johnson for testing an earlier version of this software package. This tutorial grew out of notes assembled from communications with him in 2014.

Bibliography

Komatitsch, D. and Tromp, J., Introduction to the spectral element method for three-dimensional seismic wave propagation. *Geophys. J. Int.*, 139, 806-822 (1999).

Pollitz, F.F., Gravitational viscoelastic postseismic relaxation on a layered spherical Earth, *J. Geophys. Res.*, 102, 17921-17941 (1997).

Pollitz, F. F., Post-earthquake relaxation using a spectral element method: 2.5-D case, *Geophys. J. Int.*, doi: 10.1093/gji/ggu114 (2014).

Pollitz, F.F., Post-earthquake relaxation evidence for laterally variable viscoelastic structure and water content in the southern California mantle, *J. Geophys. Res.*, 120, 2672-2696, doi:10.1002/2014JB011603 (2015).

Sinclair, C., Greenhalgh, S., and Zhou, B., 2.5D modeling of elastic waves in transversely isotropic media using the spectral element method, *Exploration Geophysics*, 38, 225-234 (2007).

1 Introduction

VISCO2.5D is a software package to calculate quasi-static deformation resulting from imposed earthquake sources in a spherical geometry. It solves the 3D equations of quasi-static equilibrium using the spectral element method (SEM) on a two-dimensional structure, with imposed source and domain boundary conditions. The viscoelastic structure is assumed to be azimuthally symmetric about a pole of symmetry (typically very distant from the model domain, in which case the structure practically varies in one horizontal Cartesian coordinate). In the spectral element domain, it produces time-dependent displacements at sets of points on Earth's surface and vertical profiles, as well as specified 'receiver' locations.

The program package is intended as a tool in modeling postseismic crustal deformation in the case that the sub-lithosphere rheology may be approximated with a linear stress-strain relation and the viscoelastic structure is two-dimensional. Such 2D structures would correspond to a contrast in material properties across, e.g. a long strike slip fault or a long convergent plate boundary with a dipping downgoing plate.

2 Description of program

The main program visco2pt5d is used for all steps of the computations needed to define a 2D global grid, specify a 2D viscoelastic structure, compute 3D postseismic displacements at various points in the model domain in the Laplace transform domain, and obtain time domain results.

Pollitz (2014) adapted the SEM of Komatitsch and Tromp (1999) for seismic wave propagation to the case of quasi-static motions. For the 2.5D problem, the approach is essentially that of Sinclair et al. (2007) adapted to the case of quasi-static deformation and a spherical geometry.

Following Pollitz (2014), the steps involved with calculating 2.5D quasi-static deformation are:

- (1) Define a 2D set of quadrilateral elements and derive a global indexing of this grid
- (2) Use the strong form of the equations of quasi-static equilibrium
- (3) Discretize the model
 - mesh of elements
 - obtain transformation between physical and local elemental coordinates
- (4) Interpolate functions on the elements
 - Lagrange polynomials
 - Gauss-Lobatto-Legendre (GLL) points
- (5) Integrate over individual elements
 - GLL integration quadrature
 - GLL points and weights
- (6) Define stiffness matrix
- (7) Assemble global linear system
- (8) Solve for displacements at the GLL points as a function of azimuthal order number
- (9) Perform weighted sum over azimuthal order, the weights depending on the azimuth of a given observation point
- (10) Inverse Laplace transform to obtain time domain results.

Generally, three runs of visco2pt5d in sequence accomplish these steps. The first run accomplishes step (1), the second run steps (2) through (8), and the third run step (9).

We work in a $r - \theta - \phi$ spherical coordinate system (hereafter ‘model coordinates’). A 2D spectral element domain is defined with respect to spherical coordinates of radius r and angular distance θ from a pole of symmetry P . Laterally variable 3D viscoelastic structure depends only upon r and θ , i.e., it is azimuthally symmetric. A seismic point source is implemented with an assumed periodicity in longitude ϕ with respect to P . The computational domain occupies a vertical slice bounded by a spherical shell at depth, the free surface, and vertical surfaces at two given angular distances from P .

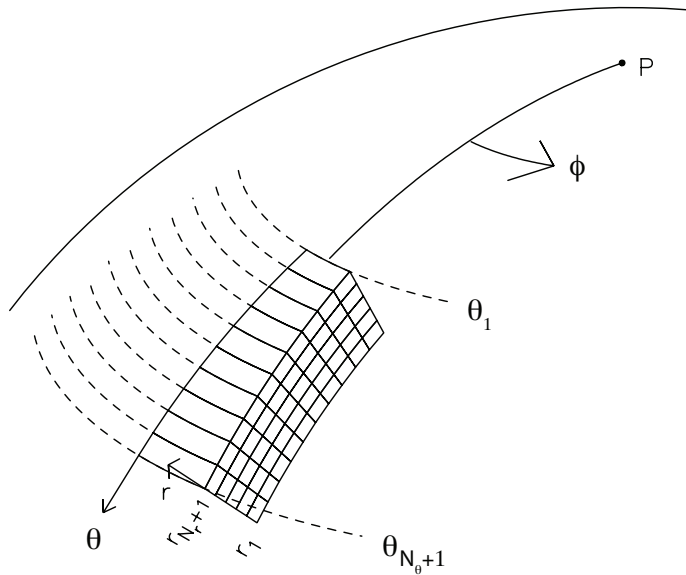


Figure 1. Geometry of model domain in 2.5D. Viscoelastic structure is assumed symmetric with respect to a symmetry pole P, i.e., it does not vary with ϕ , but may vary with θ and r . There are N_θ and N_r divisions of the model domain in the θ and r coordinates, respectively. Figure 1 of Pollitz (2014).

The viscoelastic structure and corresponding 2D GLL grid used in a typical run (e.g. Example 1 of this tutorial) looks like

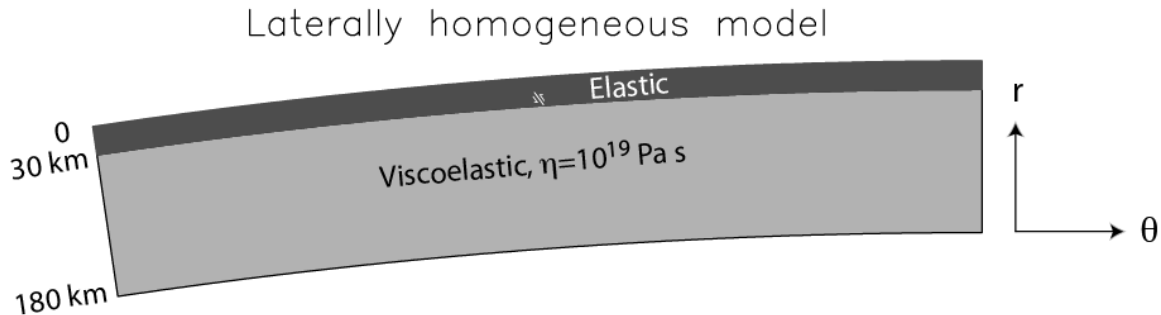


Figure 2. Definition of a 2D model domain into an elastic upper layer underlain by a viscoelastic medium.

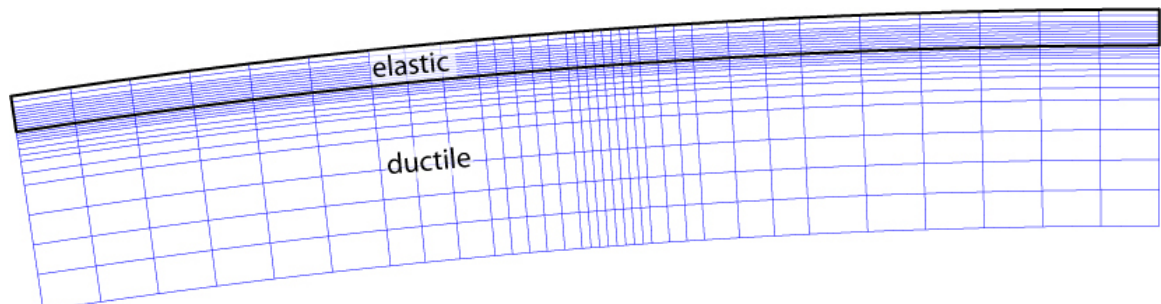


Figure 3. Division of 2D model domain into elements that are rectangular in r - θ space.

The present implementation uses rectangles in r - θ space to represent individual elements, i.e., different radius levels are separated by spherical shells, and angular distances are discretized with

the same spacing regardless of radius.

An individual element is discretized with GLL points, which serve as both collocation points for displacement and interpolation points for integrating the weighted equations of equilibrium over an element. For example, for 1D GLL functions of order $N=5$ in one dimension, the 2D GLL Cartesian grid looks like

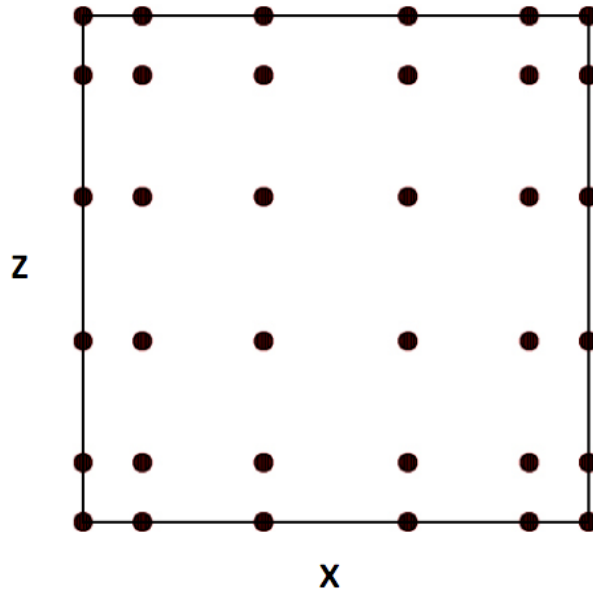


Figure 4. 2D GLL interpolation and quadrature points of one element.

There is a simple mapping between (x, z) in elemental coordinates and (θ, r) in physical spherical coordinates (eqns 17 and 18 of Pollitz, 2014). If there are $N+1$ points on the side of an element, then there are altogether $(N N_r + 1)(N N_\theta + 1)$ points in the global domain.

The equations of quasi-static equilibrium are formulated in the Laplace transform domain in order to facilitate the implementation of an assumed linear viscoelastic rheology. Letting s represent the Laplace transform parameter, the Burgers body rheology is represented with s -dependent bulk modulus κ_1 equal to the elastic bulk modulus κ and s -dependent shear modulus given by

$$\mu(s) = \frac{\mu_1 s \left(s + \frac{\mu_2}{\eta_2} \right)}{\left[\left(s + \frac{\mu_2}{\eta_2} \right) \left(s + \frac{\mu_1}{\eta_1} \right) + s \frac{\mu_1}{\eta_2} \right]}$$

where μ_1 and μ_2 are the shear modulus of the Maxwell and Kelvin elements, respectively, and η_1 and η_2 are the viscosity of the Maxwell and Kelvin elements, respectively.

The displacement field $u(r, \theta, \phi; s)$ for a given s is parameterized with expansion coefficients evaluated at the 2D GLL collocation points. This displacement field depends on model radius r , colatitude θ , and longitude ϕ .

Assuming there is a global mapping between local coordinates x,z in an element and latitude and

longitude in global model coordinates, the ϕ dependence is realized with a sum over azimuthal order number m .

$$\mathbf{u}(r, \theta, \phi; s) = \sum_{m=-\infty}^{\infty} \sum_{\alpha=0}^N \sum_{\beta=0}^N \left[a_{\alpha\beta}^m(s) \psi_{\alpha\beta}(x, z) \hat{\theta} + b_{\alpha\beta}^m(s) \psi_{\alpha\beta}(x, z) \hat{\phi} + c_{\alpha\beta}^m(s) \psi_{\alpha\beta}(x, z) \hat{\mathbf{r}} \right] e^{im\phi} \quad (1)$$

where

($a_{\alpha\beta}^m$, $b_{\alpha\beta}^m$, and $c_{\alpha\beta}^m$)

are expansion coefficients for displacement and the Ψ -functions are 2D GLL functions, e.g. Appendix A of Pollitz (2014).

There are three sets of displacement expansion coefficients, one for each of the local unit vector directions at a given location. Thus there are altogether $3(N N_r + 1)(N N_\theta + 1)$ unknown expansion coefficients. The linear system of simultaneous equations that results from manipulating the strong form of the equations of quasi-static equilibrium is derived in Pollitz (2014). For a given Laplace transform parameter, this system is solved for these expansion coefficients.

At the GLL points themselves,

$$\psi_{\alpha\beta}(x_\gamma, x_\nu) = \delta_{\alpha\gamma} \delta_{\beta\nu} \quad (2)$$

so that the displacement field at GLL points $(r_{\gamma\nu}, \theta_{\gamma\nu})$ and arbitrary ϕ is

$$\mathbf{u}(r_{\gamma\nu}, \theta_{\gamma\nu}, \phi; s) = \sum_{m=-\infty}^{\infty} \left[a_{\gamma\nu}^m(s) \hat{\theta} + b_{\gamma\nu}^m(s) \hat{\phi} + c_{\gamma\nu}^m(s) \hat{\mathbf{r}} \right] e^{im\phi} \quad (3)$$

Equation (1) is used by visco2pt5d to output static and time-dependent postseismic displacements at Earth's surface or at selected receiver points.

Equation (3) is used by visco2pt5d to output static and time-dependent postseismic displacements on a vertical profile along a chosen arc of constant longitude (presently, this is hardwired in the source code to be the arc $\phi=0$).

3 Checklist of input parameters

All of the information below must be specified in the various input files used in VISCO2.5D.

Earth model

- Viscoelastic structure as a function of depth and one lateral distance: density ρ , seismic wavespeeds V_p and V_s (equivalent to bulk modulus κ and shear modulus of Maxwell element μ_1), shear modulus of Kelvin element μ_2 , Maxwellian viscosity η_1 , and Kelvin viscosity η_2 as a function of radius. μ_2 is prescribed indirectly through the strength construct $\mu' = \mu_1 \mu_2 / (\mu_1 + \mu_2)$
- Radius of Earth

Source model

- Number of fault planes
- Strike, dip, rake, slip, length, depths of upper and lower fault edges, latitude and longitude of one fault corner
- Earthquake origin time; start and end times of cumulative postseismic displacements
- (Optional) Observation points to output displacements - in addition to GLL points**
- Number of observation points
- Latitude, longitude, and depth of these observation points

4 Compiling

Folders OpenBLAS-0.3.13, AMD, Suitesparse, and UMFPACK comprise the linear algebra package needed to compile VISCO2PT5. They are in the VISCO2.5D folder. All but OpenBLAS were originally obtained as the package SuiteSparse v4.4.4 downloaded from <http://faculty.cse.tamu.edu/davis/suitesparse.html>

This package is due to Timothy A Davis: <http://faculty.cse.tamu.edu/davis/publications.html>

The configuration file VISCO2.5D/ SuiteSparse_config/SuiteSparse_config.mk has been modified for our application.

gfortran must be installed in order to compile libraries and main programs.

AMD, Suitesparse, and UMFPACK libraries need to be compiled before the main program can be compiled. The names of the desired libraries are

VISCO2.5D/OpenBLAS-0.3.13/libopenblas.a

VISCO2.5D/Suitesparse/AMD/Lib/libamd.a

VISCO2.5D/Suitesparse/SuiteSparse_config/libsuitesparseconfig.a

VISCO2.5D/Suitesparse/UMFPACK/Lib/libumfpack.a

- Compile AMD, OpenBLAS-0.3.13, Suitesparse, and UMFPACK libraries.

Change directory to VISCO2.5D/MAINPROG

Type 'make libs'

- Edit the file VISCO2.5D/SuiteSparse/SuiteSparse_config/SuiteSparse_config.mk

In the line that reads

BLAS = /Users/fpollitz/fred4/CIDER2015/SEIS2.5D/OpenBLAS-0.3.13/libopenblas.a

Replace the right hand side with the path to that library on your machine.

- Compile visco2pt5d

In VISCO2.5D/MAINPROG

Type 'make visco2pt5d'

The above make is for 64 bit. You may need to type in

make umf4_f77zwrapper64.o

before you try

make visco2pt5d

5 Examples

The examples given here are abbreviated descriptions of how to compute post-earthquake

deformation for single-plane ruptures. Before running the examples, compile visco2pt5d as directed above.

5.1 Example 1

This example will do all of the calculations necessary to replicate Figure 6-8 of Pollitz (2014), which evaluates post-strike-slip faulting displacements generated by a 50 km-long vertical fault occupying the lower portion of the elastic layer on a spherically-layered model. This model has a prescribed Maxwell viscoelastic asthenosphere below an elastic lithosphere. Results include the $t = 1, 2$, and 5τ curves of Pollitz (2014, Figure 8), where τ is defined as $\tau = 2 \eta_1 / \mu_1$.

To run this example, run the command file ‘example1.x’, which contains the lines

```
#!/bin/bash
#
export VISCODIR=/home/cig/VISCO2.5D
export EXDIR=$VISCODIR/MAINPROG
export WORKDIR=$VISCODIR/Work
export WORKDIR1=$VISCODIR/Work1
#
cp elastic.paramEX1-Maxwell $WORKDIR/elastic.param
cp simulation-spherical.infoEX1 $WORKDIR/simulation-spherical.info
cp source-spherical.paramEX1 $WORKDIR/source-spherical.param
cp $EXDIR/visco2pt5d $WORKDIR/.

cd $WORKDIR
\rm sporder.out
./visco2pt5d << !
1
!

date > $WORKDIR1/visco2pt5d-progress1.txt

cp $WORKDIR/elastic.param $WORKDIR1/.
cp $WORKDIR/simulation-spherical.info $WORKDIR1/.
cp $WORKDIR/source-spherical.param $WORKDIR1/.
cp receivers-latlondepEX1.txt $WORKDIR/receivers-latlondep.txt
cp $EXDIR/visco2pt5d $WORKDIR1/.

cd $WORKDIR1
ln -sf $WORKDIR/sporder.out sporder.out
cp $WORKDIR/receivers-latlondep.txt receivers-latlondep.txt
./visco2pt5d << ! > /dev/null
0
rec-j-m1
displ-j-m1
visco2pt5d-progress1.txt
0. 1.00
!
```

```

cd $WORKDIR
cp $WORKDIR1/vertp-j vertp-j
cp $WORKDIR1/rec-j-m1 rec-j-m
cp $WORKDIR1/displ-j-m1 displ-j-m

./visco2pt5d << ! > /dev/null
2
not-needed
not-needed
not-needed
0. 1.00
!
#
mv visco2pt5d-stat_vertp.gmt visco2pt5d-stat_vertp-EX1.gmt
mv visco2pt5d-statstrains_vertp.gmt visco2pt5d-statstrains_vertp-EX1.gmt
mv visco2pt5d-stat-rec.gmt visco2pt5d-stat-rec-EX1.gmt
mv visco2pt5d-statstrains-rec.gmt visco2pt5d-statstrains-rec-EX1.gmt
mv visco2pt5d-post_vertp.gmt visco2pt5d-post_vertp-EX1.gmt
mv visco2pt5d-poststrains_vertp.gmt visco2pt5d-poststrains_vertp-EX1.gmt
mv visco2pt5d-post-rec.gmt visco2pt5d-post-rec-EX1.gmt
mv visco2pt5d-poststrains-rec.gmt visco2pt5d-poststrains-rec-EX1.gmt
mv visco2pt5d-stat-phival.gmt visco2pt5d-stat-phival-EX1.gmt
mv visco2pt5d-post-phival.gmt visco2pt5d-post-phival-EX1.gmt

```

Explanation of example1.x:

The first line, which specifies VISCODIR, sets the directory from where the example is being launched. 'example1.x' (and similarly 'example2.x' and 'example3.x') must be edited and this first line changed to the appropriate directory on the user's machine, i.e., where the EXAMPLES-VISCO2.5D directory resides.

EXDIR is the directory where a compiled version of visco2pt5 resides.

WORKDIR and WORKDIR1 are working directories where visco2pt5d is executed.

In a first step, relevant input files are copied to the WORKDIR directory. Then visco2pt5d is run in the WORKDIR directory with '1' in standard input. This tells it to only work on various indexing arrays that define the global grid.

In a second step, relevant input files are copied to the WORKDIR1 directory. Then visco2pt5d is run in the WORKDIR1 directory with '0' in standard input. This generates displacements of several types in the Laplace transform domain. This includes deformation at a specified set of receivers, on a vertical profile corresponding to azimuth=0 in model coordinates, and on Earth's surface.

In a third step, several files which contain Laplace-transformed displacements are copied from the WORKDIR1 directory to the WORKDIR directory. Then visco2pt5d is run in the WORKDIR

directory with '2' in standard input. This converts the Laplace-transformed displacements to time-dependent displacements and written to various output files which are finally in the WORKDIR directory.

visco2pt5d-stat_vertp.gmt has static displacements on a vertical profile corresponding to azimuth=0 in model coordinates.

visco2pt5d-statstrains_vertp.gmt has corresponding static strain components.

visco2pt5d-stat-rec.gmt has static displacements at the receiver points.

visco2pt5d-statstrains-rec.gmt has static tensor strain components at the receiver points.

visco2pt5d-stat-phival.gmt gmt has static displacements and free air gravity anomaly at a set of points on Earth's surface that encompasses the azimuth=0 in model coordinates.

visco2pt5d-post-rec.gmt has postseismic displacements at the receiver points. These are the post seismic cumulative displacements from time 0 up to a set of ten times following the synthetic earthquake.

visco2pt5d-poststrains-rec.gmt has the corresponding postseismic tensor strains at the receiver points.

visco2pt5d-post_vertp.gmt has postseismic displacements on a vertical profile corresponding to azimuth=0 in model coordinates. These are the post seismic cumulative displacements up to a set of ten times following the synthetic earthquake.

visco2pt5d-poststrains_vertp.gmt has corresponding postseismic strain components.

visco2pt5d-post-phival.gmt gmt has postseismic displacements and free air gravity anomaly at a set of points on Earth's surface that encompasses the azimuth=0 in model coordinates. These are cumulative postseismic displacements from time 0 up to times $1, 2, \dots, 5 \tau$ after the synthetic earthquake.

In a final step, these output files are moved to files with names designating Example 1.

Note that the computed static displacements are generally not going to be accurate because the minimum wavelength of the computation of 30 km (specified in **simulation-spherical.info** in this example) is too long for the static displacement field, but this minimum wavelength is sufficient for the post-earthquake relaxation calculations.

Explanation of input files:

(1) Annotated version of **simulation-spherical.infoEX1**, including the format of viscoelastic model parameter file **elastic.paramEX1-Maxwell**

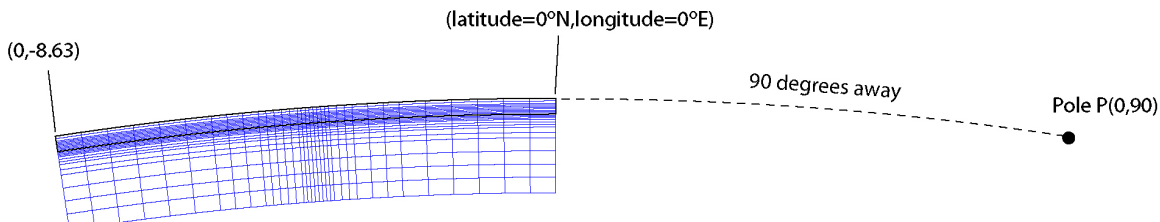


Figure 5. 2D model domain (in blue) and geometry specified in **simulation-spherical.infoEX1**.

[The model domain is essentially bounded by two small circles centered on a pole prescribed by the first two input lines (as well the radial dimension as prescribed in input lines 5-6).

In this file the pole is located 90 degrees away from (0.0N,0.0E)
at an azimuth of 90 deg. from that point. This pole is located at P=(0.0,90.0E).]

geographic coordinates of (theta,phi)=(theta_ref,0.) of spherical geometry in (deg.,deg.)

0. 0.
 # Angular distance theta_ref (geocentric deg.) and azimuth (deg. CW from due N) of pole from
 the above point
 90. 90.
 # number of cells in theta^_direction
 34

[The first small circle is defined as being 90 geocentric degrees away from P.
 The second small circle is defined as being 90 geocentric degrees + SUM_T radians away
 from P, where SUM_T is the sum of the 34 spherical-surface cell dimensions given below.
 This turns out to be SUM_T = 0.150682688 radians = 8.63348198 degrees. So the second small
 circle is 90 + 8.63348198 = 98.63348198 degrees from P.]

theta-length of each cell (radians)
 7.8480615e-3 7.8480615e-3 7.8480615e-3 7.8480615e-3 7.8480615e-3 7.8480615e-3
 4.7088369e-3 4.7088369e-3 4.7088369e-3 2.354418e-3 2.354418e-3 2.354418e-3 1.17720e-3
 1.17720e-3 1.17720e-3 1.17720e-3 1.17720e-3 1.17720e-3 1.17720e-3 2.354418e-3
 2.354418e-3 2.354418e-3 2.354418e-3 2.354418e-3 4.7088369e-3 4.7088369e-3 4.7088369e-3
 7.8480615e-3 7.8480615e-3 7.8480615e-3 7.8480615e-3 7.8480615e-3 7.8480615e-3
 # number of cells in z-direction
 23

[There are 23 cells in the radial direction, going from a depth of SUM_Z to earth's surface,
 where SUM_Z is the sum of the 23 radial cell dimensions given below.
 This yields SUM_Z = 180 km, corresponding to a radius of 6371 - 180 = 6191 km.
 The cell size is taken larger at greater depth, i.e. the first one in the radial dimension goes
 from 180 to 150 km depth, the next from 150 to 125 km, the next from 125 to 100 km, etc.
 Note that the actual computational domain is 2D
 and goes from 0 to 0.150682688 radians in theta and 6191 to 6371 km in radius.
 The theta computational domain is best thought of as being along an azimuth $\phi=0$ defined
 by the great circle connecting P with the given point (0.0N,0.0E) on the first small circle.
 This great circle intersects the second small circle at (0.0N,-8.63348198E). So the 2D
 computational domain is bounded - in theta - by an arc connecting (0.0N,0.0E) with (0.0N,-
 8.63348198E) and - in radius - by spherical shells at 180 and 0 km depth.]

z-length of each cell (km)
 30. 25. 25. 25. 10. 10. 5. 5. 2.5 2.5 2.5 2.5 2.5 2.5 2.5 2.5 2.5 2.5 2.5 2.5 2.5 2.5 5.0 5.0
 # Effective width of third (i.e. phi) dimension (km); minimum wavelength in third dimension
 (km)

[For computational speedup, we suppose that there are sources evenly distributed in azimuth from
 P; the spacing between successive sources is 1200 km. This implemented in a spherical geometry
 by stepping in azimuthal order number by an amount approximately equal to
 $2\pi / (1200 \text{ km} * \sin(90. \text{ deg})) = 33$. Similarly, with the 20. km minimum
 wavelength prescribed below, the maximum azimuthal order number used in the computation is
 $2\pi / (30 \text{ km} * \sin(90. \text{ deg})) = 1333$. The minimum azimuthal order number is 0.]

1200. 30.
 # input file with elastic parameters

[This file has pointwise values of seismic velocities and Maxwell-solid parameters with the

format

theta (deg.)	r-6371. (km)	Vp (km/s)	Vs (km/s)	Rho (g/cm ³)	\mu' (10 ^{10} Pa)	\eta_2 (10 ^{18} Pa s)	\eta_1 (10 ^{18} Pa s)
0.0000	-180.0000	5.4772	3.1623	3.0000		0.100000E+02	
0.0000	-177.0002	5.4772	3.1623	3.0000		0.100000E+02	
0.0000	-174.0004	5.4772	3.1623	3.0000		0.100000E+02	

(sample lines)

theta is measured positive from (0.0N,0.0E) along the great circle connecting P and that point, i.e., along the azimuth 90-180 = -90 deg. from (0.0N,0.0E). So theta=8.63348198 degrees corresponds to the point (0.0N,-8.63348198E).

r-6371 is 0 at earth's surface and -180 at the base of the computational model domain. The example file 'elastic.paramEX1-Maxwell', which is copied to elastic.param prior to running the main program, may permissibly go further down than 180 km. A simple scheme for identifying the closest point in this input file is used to assign viscoelastic parameters to the GLL points.

Vp and Vs are P-wave and S-wave isotropic seismic velocities; Rho is density.

For a Burgers body, \eta_2 and \mu_2 are the viscosity and shear modulus of the Kelvin element (transient viscosity and shear modulus), and \eta_2 and \mu_2 are the viscosity and shear modulus of the Maxwell element

(steady state viscosity and shear modulus). The seismic velocities and rho together determine the elastic bulk modulus and shear modulus \mu_1. \mu' is defined as

$$\mu' = (\mu_1 * \mu_2) / (\mu_1 + \mu_2).$$

Note that for a Maxwell solid, one can either assign \mu'=\mu_1, \eta_2=arbitrary, and \eta_1=Maxwell viscosity or equivalently, assign \mu'=0, \eta_1=very large, and \eta_2=Maxwell viscosity, or, as is done in the example file, omit \mu' and \eta_2 and provide only \eta_1.]

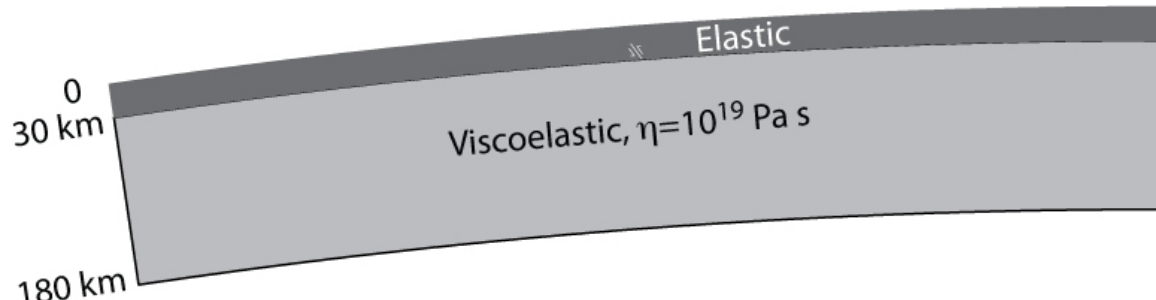


Figure 6. Laterally homogeneous model used in Example 1.

elastic.param

gravitational acceleration at earth's surface (m/s) (0 for non-gravitational case)

[In computations without gravitation, this is set to 0; in computations with gravitation, this is set to 9.8]

0.

compute free-air gravity anomaly (y or n)

y

(2) Annotated version of **source-spherical.paramEX1**

[cumulative postseismic displacements are evaluated in most cases from time t_1 to t_2 from an earthquake source at time t_0 , where t_0 is the year of earthquake, t_1 is the year obs. #1, and t_2 is year obs. #2. The viscosity multiplier has the effect multiplying all viscosities in the prescribed viscoelastic model by the given number. It is set to unity in these examples.]

```
# year of earthquake, year obs.#1, year obs.#2 (yrs), viscosity multiplier  
1975. 1975. 1996.164 1.  
# finite fault with # segments  
1  
# max depth, min depth (km), dip(deg.)  
# lat,lon(deg.),length(km),strike(deg.),rake(deg.),slip(cm) for each segment  
29.00 15.00 90.  
0.1589861 -4.15000 50. 45. 180. 100.
```

[This last line specifies the fault geometry of a dislocation plane.
The lower edge depth is 29.00 km, upper edge depth is 15.00, dip=90 deg.
30.1589861 -4.15000 is the lat,lon of the point on the lower edge of the fault closest to the strike direction, which is 45 deg.=N45E. That is, it is the northernmost point on the lower edge.
The fault length is 50 km, rake is 180.0 (right-lateral slip), slip is 100 cm. The conventions for strike, dip, and rake are the standard ones (e.g., Aki and Richards, 1980, p. 106).]

[The fault plane is represented with 17 x 25 point sources uniformly distributed on the plane.]

```
# along-strike discretization  
17  
# down-dip discretization  
25
```

Explanation of output files:

The first few lines of the output file **visco2pt5d-post-rec-EX1.gmt** (postseismic displacements at specified receiver locations) are:

0.0000000000000000	3.1745999999999981	-8.2377272
-2.0000000	0.0000000	5.56773576659561265E-005 4.54461572682330619E-005 -1.29277196E-005
0.0000000000000000	5.2955519653953029	-8.2377272
-2.0000000	0.0000000	9.50847334044079234E-005 7.34914490303044263E-005 -2.16601020E-005
0.0000000000000000	8.8335130782467317	-8.2377272
-2.0000000	0.0000000	1.62315247163634943E-004 1.17579318461441591E-004 -3.63086838E-005
0.0000000000000000	14.735187911187120	-8.2377272
-2.0000000	0.0000000	2.74745778865951348E-004 1.85422442713521632E-004 -6.06737340E-005
0.0000000000000000	24.579774870395045	-8.2377272
-2.0000000	0.0000000	4.57565272964112631E-004 2.83959540628751046E-004 -1.00108082E-004
0.0000000000000000	41.001535665562479	-8.2377272
-2.0000000	0.0000000	7.44945096034685416E-004 4.08578817037272410E-004 -1.60279669E-004
0.0000000000000000	68.394683669752155	-8.2377272
-2.0000000	0.0000000	1.16527355489295719E-003 5.32394887674305208E-004 -2.43485963E-004
0.0000000000000000	114.08920857114164	-8.2377272
-2.0000000	0.0000000	1.69072748708167160E-003 6.13905229049785959E-004 -3.42537882E-004
0.0000000000000000	190.31227010625091	-8.2377272
-2.0000000	0.0000000	2.19753663813855062E-003 6.10738739345476761E-004 -4.34649031E-004

0.000000000000000	317.4599999999992	-8.2377272		
-2.0000000	0.0000000	2.51901085900534810E-003	5.24046124479864259E-004	-4.85738565E-04

Columns 1 and 2 have the time interval (years) for cumulative displacement.
 Columns 3 and 4 have the longitude and latitude of the receiver point in geographic coordinates (degrees), column 5 the (negative of the) depth (km), columns 6-8 the displacements (meters).

The output files **visco2pt5d-stat-rec-EX1.gmt** (static displacements at specified receiver locations), **visco2pt5d-post_vertp-EX1.gmt** (postseismic displacements on a vertical slice sampling all GLL points on the arc phi=0) ,and **visco2pt5d-stat_vertp-EX1.gmt** (static displacements on a vertical slice sampling all GLL points on the arc phi=0) have the same format as above.

Note that **visco2pt5d-post-rec-EX1.gmt** has cumulative displacements (columns 6,7,8 [E, N, Up displacements]) for each of 10 logarithmically-spaced postseismic time intervals at 121 receiver sites -- those in `receivers-latlondepEX1.txt'. Similarly, **visco2pt5d-post_vertp-EX1.gmt** has cumulative displacements (columns 6,7,8 [E, N, Up displacements]) for each of 10 postseismic time intervals on the profile corresponding to azimuth=0 in model coordinates.

The first few lines of the output file **visco2pt5d-post-phival-EX1.gmt** (postseismic displacements at a set of points on Earth's surface) are:

0.000000000000000	21.163999270316285	-2.50629500E-06	2.18182373	-2.9411716566840818E-004
-2.0969052230328624E-004	-7.10927270E-05	-1.35696846E-05		
0.000000000000000	42.327998540632571	-2.50629500E-06	2.18182373	-5.8328216544770921E-004
-3.5138060659956191E-004	-1.36531133E-04	-2.78012321E-05		
0.000000000000000	63.491997810948860	-2.50629500E-06	2.18182373	-8.4723015504194372E-004
-4.3880069322261688E-004	-1.91844476E-04	-4.04003877E-05		
0.000000000000000	84.655997081265141	-2.50629500E-06	2.18182373	-1.0780632742606606E-003
-4.9127927050906779E-004	-2.37672648E-04	-5.08786979E-05		
0.000000000000000	105.81999635158142	-2.50629500E-06	2.18182373	-1.2747673715648748E-003
-5.2118941770322620E-004	-2.75395752E-04	-5.93239492E-05		
0.000000000000000	21.163999270316285	-5.28586730E-02	2.18182373	-2.9744944172035488E-004
-2.1237986227951649E-004	-7.18501324E-05	-1.92193329E-05		
0.000000000000000	42.327998540632571	-5.28586730E-02	2.18182373	-5.8989070319758656E-004
-3.5577130625501940E-004	-1.37975803E-04	-3.94465023E-05		
0.000000000000000	63.491997810948860	-5.28586730E-02	2.18182373	-8.5683533878416047E-004
-4.4416524439728605E-004	-1.93868706E-04	-5.74159712E-05		
0.000000000000000	84.655997081265141	-5.28586730E-02	2.18182373	-1.0902934714611999E-003
-4.9717470194329848E-004	-2.40177673E-04	-7.23901758E-05		
0.000000000000000	105.81999635158142	-5.28586730E-02	2.18182373	-1.2892367986486511E-003
-5.2734659784998224E-004	-2.78297550E-04	-8.44724345E-05		

Columns 1 and 2 have the time interval (years) for cumulative displacement.
 Columns 3 and 4 have the longitude and latitude of the receiver point in geographic coordinates, and columns 5-7 the displacements (units are meters).
 Column 8 has the free air gravity anomaly in mGal. This gravity anomaly includes the effects of uplift of iso-density surfaces and volumetric density change due to dilatational strain.

Remarks concerning the computation of the free-air gravity anomaly:

- This example calculated free-air gravity anomaly at earth's surface according to the specification in **simulation-spherical.infoEX1**, i.e., 'y' on the last input line of that file
- *Computation time when gravity anomaly is desired is generally 4 times slower than without the gravity anomaly computation.* Most users will not wish to compute gravity anomaly and can accordingly specify 'n' in the last input line of **simulation-**

- **spherical.infoEX1** or simply do not include the last line in this input file
- In order to account for the presence of a superficial water layer, if the density of the uppermost cell for a given theta is 1.000 g-cm^{-3} , then the free-air effect of uplift of the free surface is ignored, regardless of the assigned value of elastic parameters in that cell.

Note that the observation time interval specified in **source-spherical.paramEX1** (first 21.164 years following the synthetic event) was chosen to be the 1τ postseismic interval, as dictated by the Maxwell viscosity and shear modulus of the sub-lithosphere specified in **elastic.paramEX1-Maxwell**. That is, the time interval (t_1, t_2) corresponds to cumulative displacements up to 1τ years following the slip event. This was chosen for this example so that the displacements in **visco2pt5d-post-phival-EX1.gmt** correspond to multiples of the first 1τ postseismic interval, i.e. the five output time intervals are $(0, 1\tau)$, $(0, 2\tau)$, $(0, 3\tau)$, $(0, 4\tau)$, and $(0, 5\tau)$.

The output file **visco2pt5d-poststrains-rec-EX1.gmt** (postseismic tensor strain components at specified receiver locations) has the following format:

Columns 1 and 2 have the time interval (years) for cumulative strain.

Columns 3 and 4 have the longitude and latitude of the receiver point in geographic coordinates (degrees), column 5 the (negative of the) depth (km), columns 6-11 are tensor strain components (in units of microstrain) e_EE, e_NN, e_EN, e_EZ, e_NZ, e_ZZ, where E=local East, N=local North, Z=local Up. The output files **visco2pt5d-statstrains-rec-EX1.gmt** (static strains at specified receiver locations), **visco2pt5d-poststrains_vertp-EX1.gmt** (postseismic strains on a vertical slice sampling all GLL points on the arc phi=0), and **visco2pt5d-statstrains_vertp-EX1.gmt** (static strains on a vertical slice sampling all GLL points on the arc phi=0) have the same format.

Plots

The figures below are comparisons between the visco2pt5d solutions (from output file **visco2pt5d-post-phival-EX1.gmt**) and the semi-analytic solution from viscoelastic mode summation (Pollitz, 1997). The figures correspond to Figures 6-8 of Pollitz (2014).

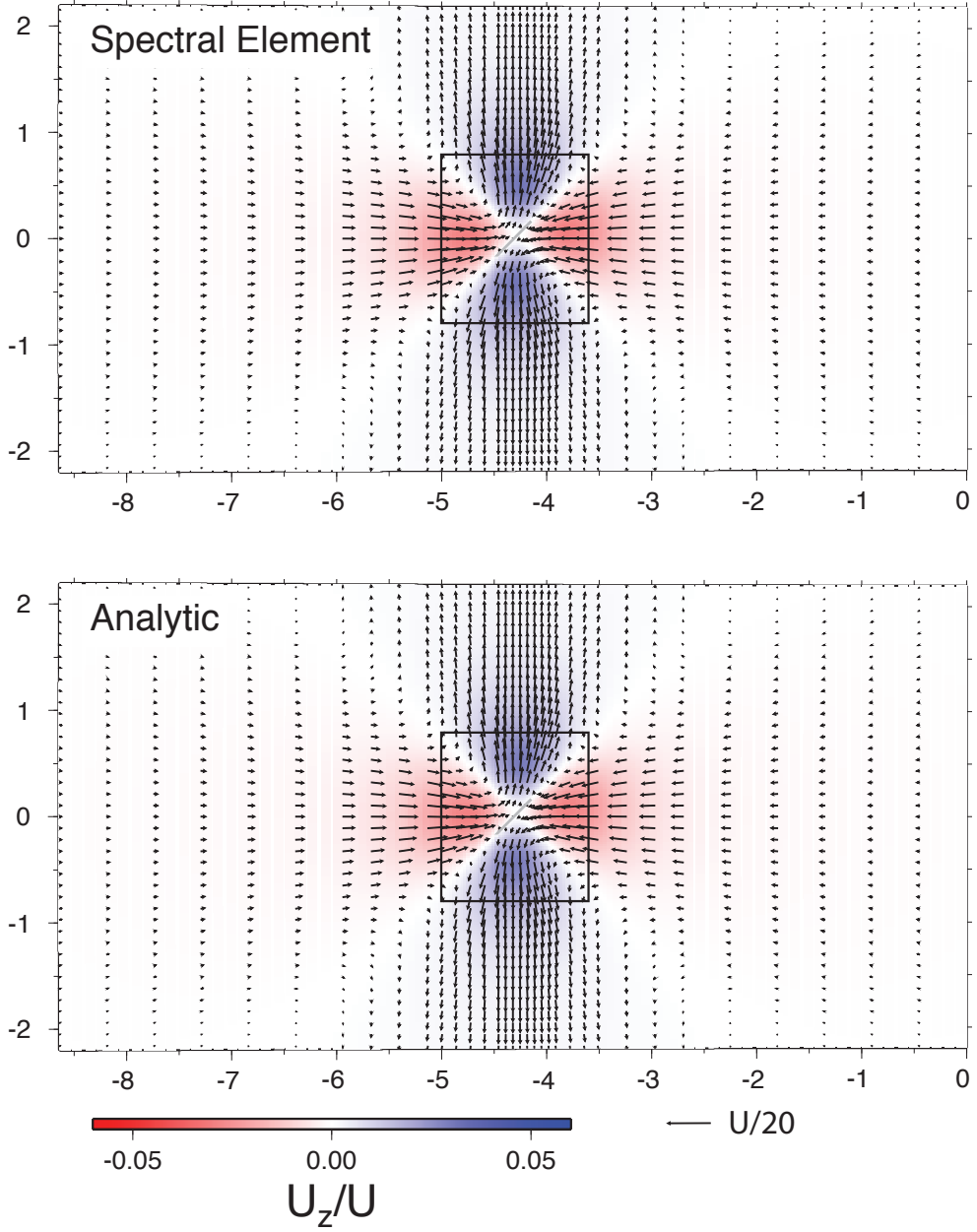


Figure 7. Horizontal displacements (arrows) and vertical displacements (color shading) for relaxation following strike-slip faulting on the fault plane indicated with the white rectangle. These are cumulative displacements up to 5τ years following the slip event, where τ is the material relaxation time of the ductile substrate. The color scale indicates the ratio of vertical displacement U_z to fault slip U . Black rectangle indicates the area plotted in Figure 8.

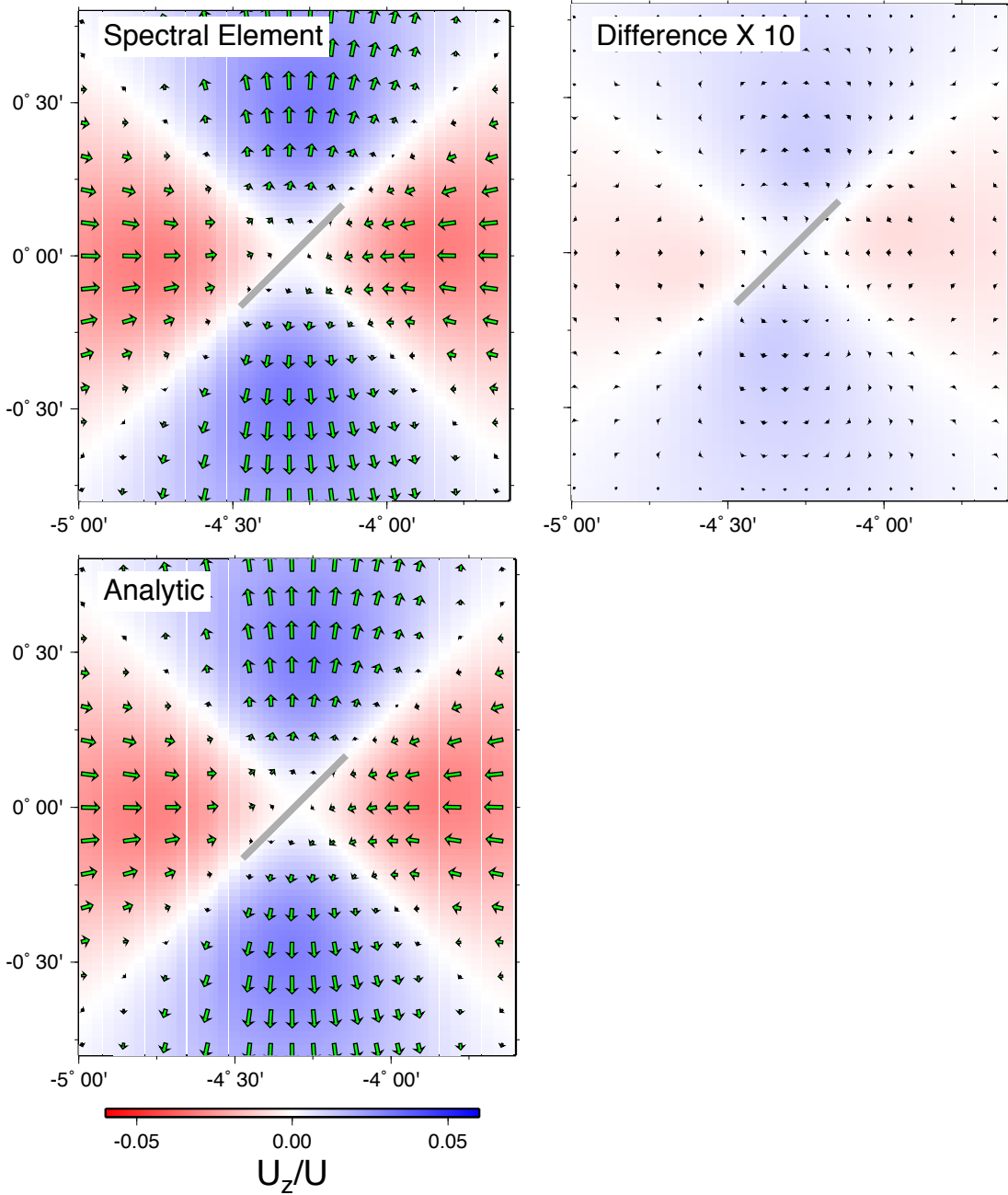


Figure 8. Close-up view of the motions following strike-slip faulting shown in Figure 7. Right-hand plot shows difference between SEM and analytic displacement fields.

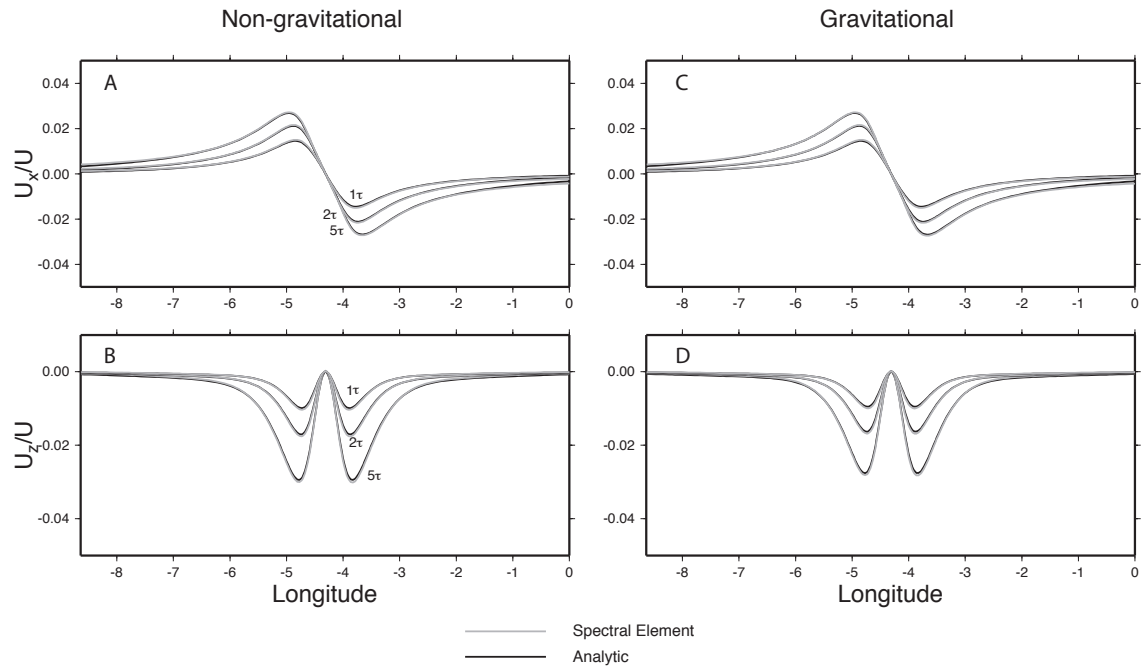


Figure 9. Ratio of horizontal displacement U_x (a,c) and vertical displacement U_z (b,d) to fault slip U for displacements following strike-slip faulting at times 1τ , 2τ , and 5τ along the equator of the area shown in Figure 7. Non-gravitational displacements from the spectral element and analytic methods are compared in a,b, and gravitational displacements in c,d.

5.2 Example 2

This example will replace the laterally homogeneous structure of Example 1 with a laterally variable structure. As in Example 1, this example evaluates post-strike-slip faulting displacements generated by a 50 km-long vertical fault occupying the lower portion of the elastic layer on a spherically-layered model. This model has a prescribed Maxwell viscoelastic asthenosphere below an elastic lithosphere. The change from Example 1 is that the lithosphere thickness has a step increase from 30 km to 100 km in the middle of the model domain.

To run this example, run the command file `example2.x', which has the same structure as `example1.x' of section 5.1, but with one different input file. This is exemplified by the first few lines of `example2.x'

```
#!/bin/bash
#
export VISCODIR=/home/cig/VISCO2.5D
export EXDIR=$VISCODIR/MAINPROG
export WORKDIR=$VISCODIR/Work
export WORKDIR1=$VISCODIR/Work1
#
cp elastic.paramEX2-Maxwell $WORKDIR/elastic.param
cp simulation-spherical.infoEX2 $WORKDIR/simulation-spherical.info
cp source-spherical.paramEX2 $WORKDIR/source-spherical.param
cp $EXDIR/visco2pt5d $WORKDIR/.
```

The input file **simulation-spherical.infoEX2** is identical to **simulation-spherical.infoEX1**, and the input file **source-spherical.paramEX2** is identical to **source-spherical.paramEX1**. The only difference with respect to Example 1 is the viscoelastic structure. The structure prescribed in the file **elastic.paramEX2-Maxwell** has pointwise values of seismic velocities and Maxwell solid parameters with the format

theta (deg.)	r-6371. (km)	Vp (km/s)	Vs (km/s)	Rho (g/cm ³)	\mu' (10 ^{10} Pa)	\eta_2 (10 ^{18} Pa s)	\eta_1 (10 ^{18} Pa s)
4.1000	-101.6098	5.4772	3.1623	3.0000		0.100000E+02	
4.1000	-100.0100	5.4772	3.1623	3.0000		0.100000E+02	
4.1000	-99.9900	5.4772	3.1623	3.0000		0.100000E+12	
4.1000	-98.5904	5.4772	3.1623	3.0000		0.100000E+12	
..							
..							
4.1872	-31.4096	5.4772	3.1623	3.0000		0.100000E+02	
4.1872	-30.0100	5.4772	3.1623	3.0000		0.100000E+02	
4.1872	-29.9900	5.4772	3.1623	3.0000		0.100000E+12	
4.1872	-29.3902	5.4772	3.1623	3.0000		0.100000E+12	

Between 4.1000 and 4.1872 degrees from the edge of the model domain, the lithosphere thickness jumps from 100 km to 30 km, as shown in Figure 10.

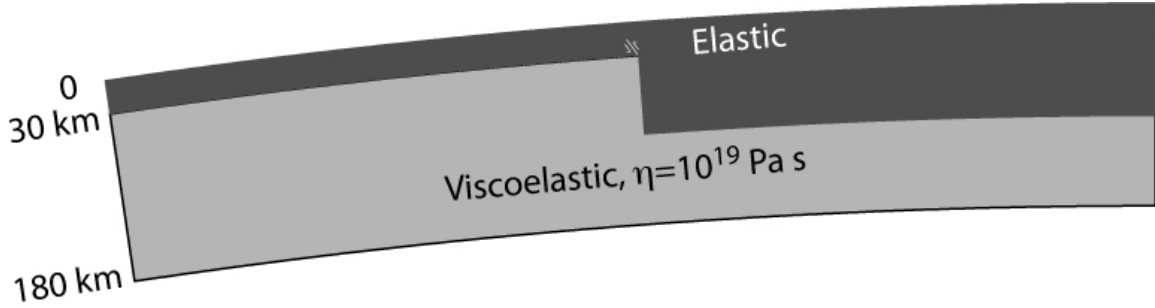


Figure 10. Laterally heterogeneous model used in Example 2.

Plots

The figures below are comparisons of surface displacements between the visco2pt5d solutions of Example 1 and Example 2. These are almost identical to Figures 13 and 14 of Pollitz (2014), but the published figures include gravitation and the present examples do not.

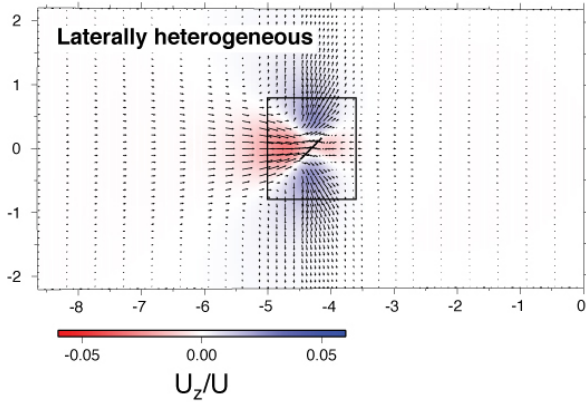
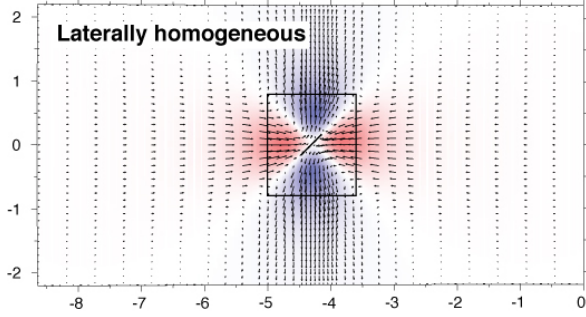


Figure 11. Horizontal displacements (arrows) and vertical displacements (color shading) for viscoelastic-gravitational relaxation following strike-slip faulting on the fault plane indicated with the black line. These are cumulative displacements up to 5τ following the slip event. The color scale indicates the ratio of vertical displacement U_z to fault slip U . The two plots compare the displacement fields on the laterally homogeneous (Example 1) and heterogeneous (Example 2) models.

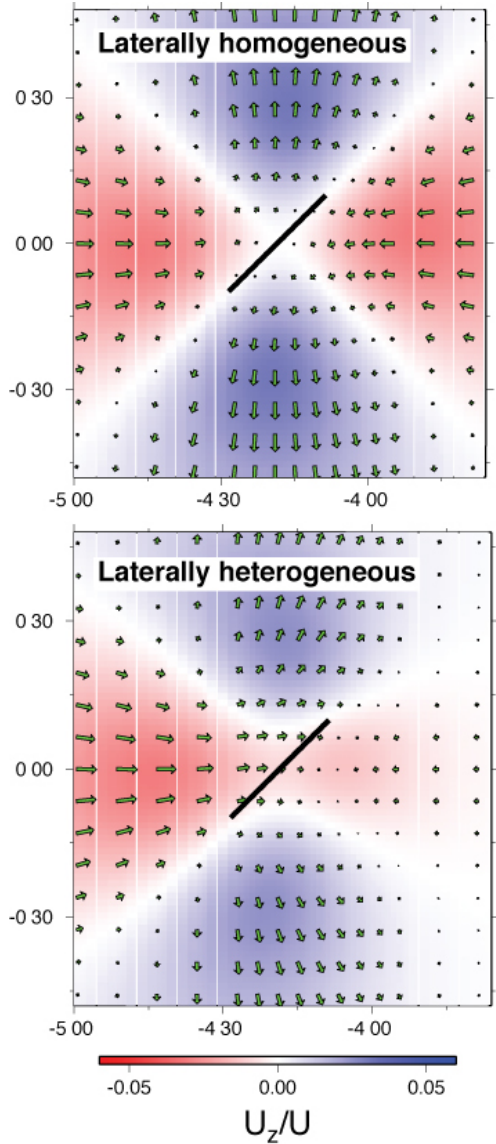


Figure 12. Zoomed-in view of the motions following strike-slip faulting shown in Figure 11.

5.3 Example 3

In this example we calculate cumulative postseismic motions following the 1999 M7.1 Hector Mine earthquake using the 2D viscoelastic structure obtained by Pollitz (2015). The viscoelastic model has a prescribed Burgers-body viscoelastic asthenosphere below an elastic lithosphere, and at mantle depths there is a discontinuity in (transient and steady-state) viscosities across a NW-SE trending boundary that divides the western and central Mojave Desert.

To run this example, run the command file ‘example3.x’, which has the same structure as ‘example1.x’ of section 5.1, just with a different set of input files. This is clear from the first few lines of ‘example3.x’

```
#!/bin/bash
#
export VISCODIR=/home/cig/VISCO2.5D
```

```

export EXDIR=$VISCODIR/MAINPROG
export WORKDIR=$VISCODIR/Work
export WORKDIR1=$VISCODIR/Work1
#
cp elastic.paramEX3 $WORKDIR/elastic.param
cp simulation-spherical.infoEX3 $WORKDIR/simulation-spherical.info
cp source-spherical.paramEX3 $WORKDIR/source-spherical.param
cp $EXDIR/visco2pt5d $WORKDIR/.

```

Explanation of input files:

(1) Annotated version of **simulation-spherical.infoEX3** (refer to Figure 13)

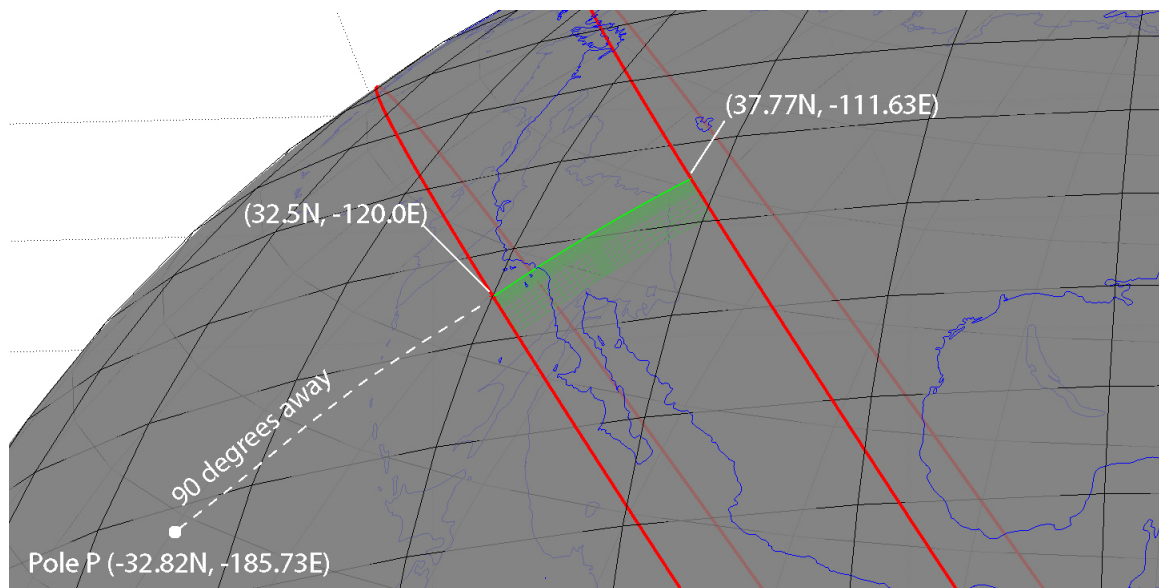


Figure 13. 2D model domain (in green) and geometry specified in **simulation-spherical.infoEX3**.

[The model domain is essentially bounded by two small circles centered on a pole prescribed by the first two input lines (as well the radial dimension as prescribed in input lines 5-6). In this file the pole is located 90 degrees away from (32.5N,-120.0E) at an azimuth of 230 deg. from that point. This pole turns out to be located at P=(-32.82N,-185.73E).]

geographic coordinates of (theta,phi)=(theta_ref,0.) of spherical geometry in (deg.,deg.)

```

32.5 -120.0
# Angular distance theta_ref (geocentric deg.) and azimuth (deg. CW from due N) of pole from
the above point
90. 230.
# number of cells in theta^_direction
34

```

[The first small circle is defined as being 90 geocentric degrees away from P.
The second small circle is defined as being 90 geocentric degrees + SUM_T radians away

from P, where SUM_T is the sum of the 34 spherical-surface cell dimensions given below. This turns out to be SUM_T = 0.150682688 radians = 8.63348198 degrees. So the second small circle is $90 + 8.63348198 = 98.63348198$ degrees from P.]

```
# theta-length of each cell (radians)
7.8480615e-3 7.8480615e-3 7.8480615e-3 7.8480615e-3 7.8480615e-3
4.7088369e-3 4.7088369e-3 4.7088369e-3 2.354418e-3 2.354418e-3 2.354418e-3
1.17720e-3 1.17720e-3 1.17720e-3 1.17720e-3 1.17720e-3 1.17720e-3
2.354418e-3 2.354418e-3 2.354418e-3 2.354418e-3 4.7088369e-3 4.7088369e-3
7.8480615e-3 7.8480615e-3 7.8480615e-3 7.8480615e-3 7.8480615e-3
# number of cells in z-direction
27
# z-length of each cell (km)
```

[There are 27 cells in the radial direction, going from a depth of SUM_Z to earth's surface, where SUM_Z is the sum of the 27 radial cell dimensions given below.

This yields SUM_Z = 300 km, corresponding to a radius of $6371 - 300 = 6071$ km.

The cell size is taken larger at greater depth, i.e. the first one in the radial dimension goes from 300 to 270 km depth, the next from 270 to 240 km, etc.

Note that the actual computation domain is 2D

and goes from 0 to 0.150682688 radians in theta and 6071 to 6371 km in radius.

The theta computational domain is best thought of as being along an azimuth phi=0 defined by the great circle connecting P with the given point (32.5N,-120.0E) on the first small circle.

This great circle intersects the second small circle at (37.77N,-111.63E). So the 2D computational domain is bounded - in theta - by an arc connecting (32.5N,-120.0E) with (37.77N,-111.63E) and - in radius - by spherical shells at 300 and 0 km depth.]

```
30. 30. 30. 30. 30. 25. 25. 10. 10. 5. 5. 2.5 2.5 2.5 2.5 2.5 2.5 2.5 2.5 2.5 2.5 2.5 2.5 2.5 5.0 5.0
# Effective width of third (i.e. phi) dimension (km); minimum wavelength in third dimension
(km)
```

[For computational speedup, we suppose that there are sources evenly distributed in azimuth from P; the spacing between successive sources is 1200 km. This implemented in a spherical geometry by stepping in azimuthal order number by an amount approximately equal to
 $\text{twopi} * 6371 \text{ km} / (1200 \text{ km} * \sin(90. \text{ deg})) = 33$. Similarly, with the 20 km minimum wavelength prescribed below, the maximum azimuthal order number used in the computation is
 $\text{twopi} * 6371 \text{ km} / (20 \text{ km} * \sin(90. \text{ deg})) = 2001$.

The minimum azimuthal order number is 0.]

1200. 20.

input file with elastic parameters

[This file has pointwise values of seismic velocities and Burgers-body parameters with the format

theta	r-6371.	Vp	Vs	Rho	\mu'	\eta_2	\eta_1
(deg.)	(km)	(km/s)	(km/s)	(g/cm^3)	(10^{10} Pa)	(10^{18} Pa s)	(10^{18} Pa s)
0.0000	-218.5601	8.4573	4.5361	3.4020	0.0000	0.100000E+03	0.100000E+14
0.0000	-216.0000	8.4573	4.5361	3.4020	0.0000	0.100000E+03	0.100000E+14
0.0000	-216.0000	8.4685	4.5421	3.3930	3.5000	0.240000E+01	0.100000E+02
0.0000	-213.4399	8.4685	4.5421	3.3930	3.5000	0.240000E+01	0.100000E+02

..

5.6702 -218.5601 8.4573 4.5361 3.4020 0.0000 0.100000E+03 0.100000E+14
 5.6702 -216.0000 8.4573 4.5361 3.4020 0.0000 0.100000E+03 0.100000E+14
 5.6702 -216.0000 8.4685 4.5421 3.3930 3.5000 0.400000E+01 0.400000E+02
 5.6702 -213.4399 8.4685 4.5421 3.3930 3.5000 0.400000E+01 0.400000E+02

This viscoelastic structure is discontinuous across a vertical boundary shown below]

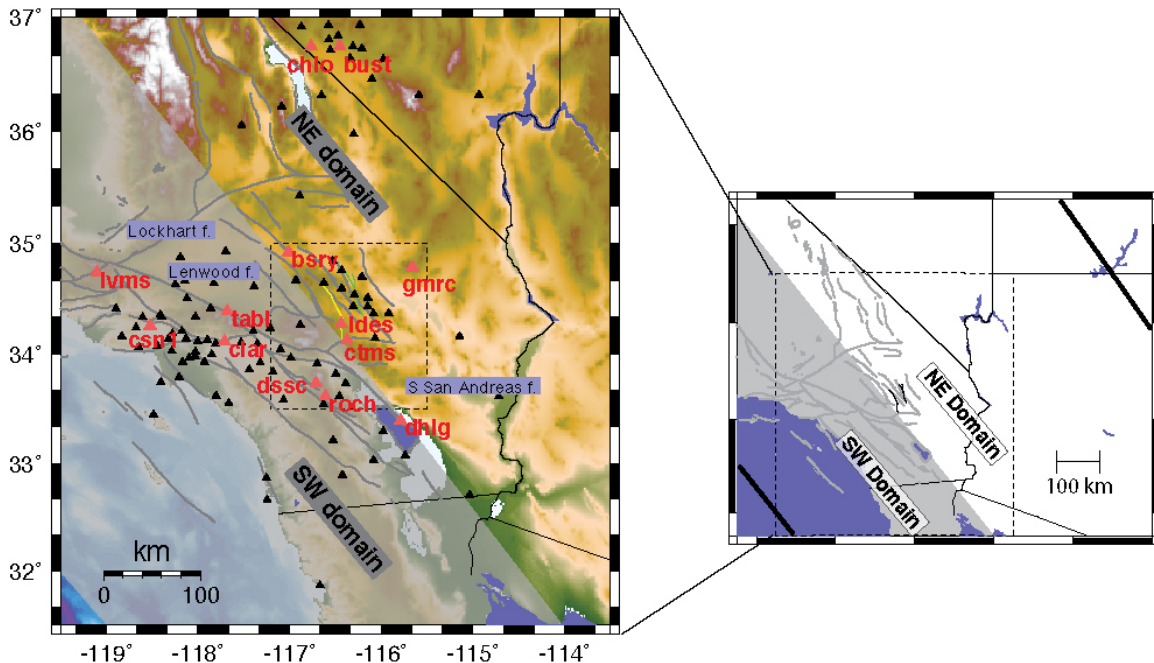


Figure 14. Definition of two structural domains in southern California having different vertical stratification of viscoelastic properties. Triangles show locations of GPS stations modeled by Pollitz (2015). Yellow and green lines denote the traces of the 1992 Landers and 1999 Hector Mine earthquake ruptures, respectively. The horizontal boundaries of the model domain are shown in the right-hand figure as thick black lines. Modified from Figure 1 of Pollitz (2015).

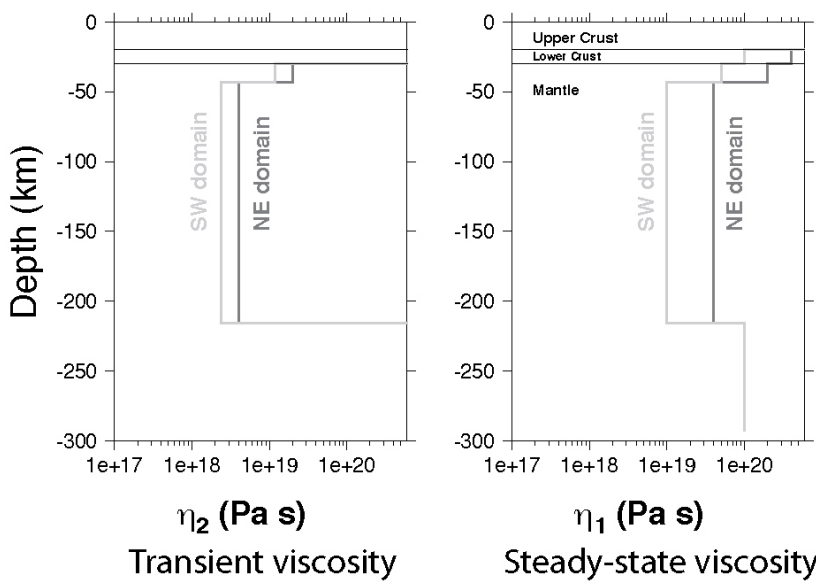


Figure 15. Depth-dependent transient (left-hand side) and steady-state (right-hand side) viscosity as a function of depth in the two domains. These structures are prescribed by visco2pt5d input file **elastic.param** (linked to **elastic.paramEX3**). Modified from Figure 9 of Pollitz (2015).

```
elastic.param
# gravitational acceleration at earth's surface (m/s^2) (0 for non-gravitational case)
```

[In computations without gravitation, this is set to 0; in computations with gravitation, this is set to 9.8]

0.

Plots

The figure below is derived from the output file **visco2pt5d-post_vertp-EX3.gmt**

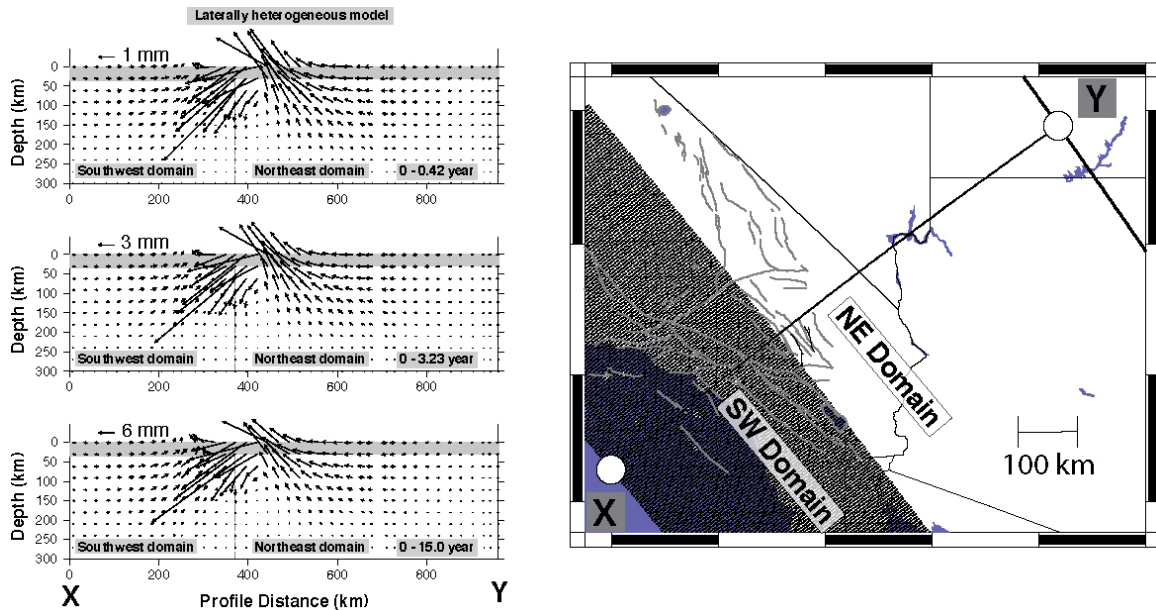


Figure 16. Cumulative post-Hector Mine displacements for the indicated time periods resolved onto a vertical plane with surface trace shown in the right-hand figure. These displacements are calculated on the 2D viscoelastic structure of Figures 12 and 13. Shaded region delineates the crust. Modified from Figure S7 of Pollitz (2015).

The figure below is the coseismic displacement field. It is plotted from the output file **visco2pt5d-stat-rec-EX3.gmt**

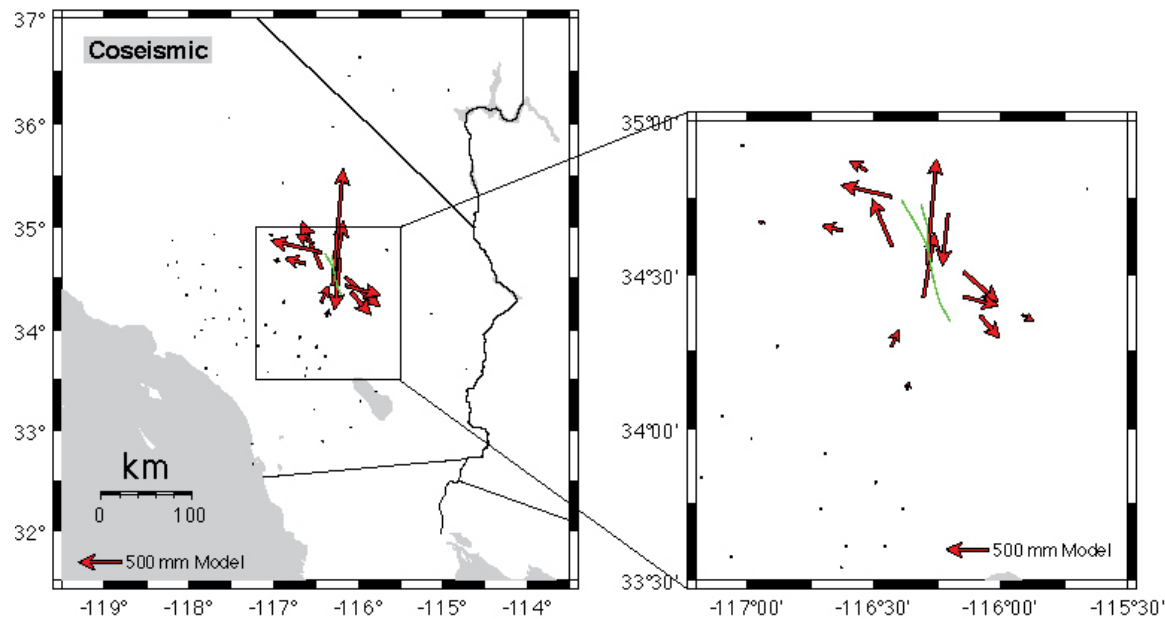


Figure 17. Coseismic displacement field at selected GPS sites for the Hector Mine earthquake generated by 'example3.x'.

The figure below is the 0 – 15 years postseismic displacement field. It is plotted from the output file **visco2pt5d-post-rec-EX3.gmt**

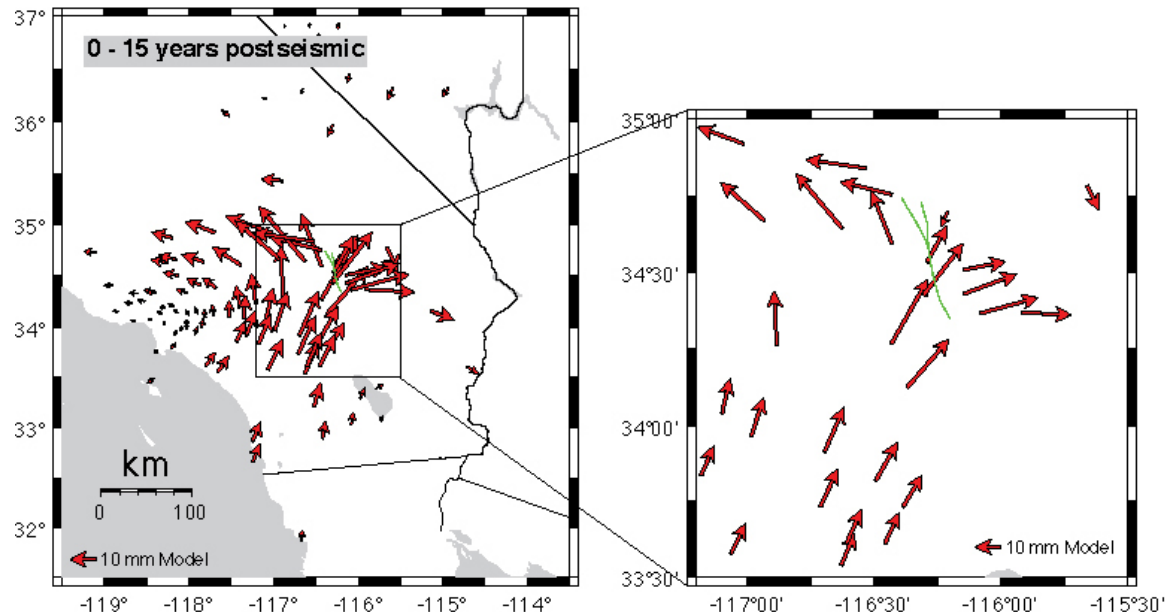


Figure 18. Postseismic displacement field at selected GPS sites for the Hector Mine earthquake generated by 'example3.x'.

6 Practical considerations

- As described in section 5.1 ("Explanation of 'example1.x'") visco2pt5d is typically run three times in sequence. The first run uses information from **simulation-spherical.info**

to obtain indexing arrays of GLL points on the global grid. Once this is done, the second and third runs determine displacements in the Laplace transform domain and time domain, respectively, using additional input files **elastic.param** and **source-spherical.param**, which are linked to specific input files in the examples of section 5. However, if the lines specifying the number of cells in the theta[^]-direction and z-direction in **simulation-spherical.info** do not change, then the first run of visco2pt5d need not be repeated. The second and third runs can be repeated with other linked files **elastic.param** and **source-spherical.param** without having to re-determine the indexing arrays.

- In the source programs (VISCO2.5D/SOURCE/) `visco2pt5d.f` and `visco2pt5dsubs.f`, parameters NCMAX and NCMAZ specify the maximum expected values of the “number of cells in theta[^]-direction” and “z-length of each cell (km)” input in **simulation-spherical.info**. The present values of NCMAX and NCMAZ are set at 37, i.e.

```
parameter (ncmax=37)
parameter (ncmaz=37)
```

If a greater number of cells in the horizontal (i.e. theta[^]) or vertical (i.e. z) directions are intended, then these parameter values should be increased within the source files (and those two lines appear several times...) and then visco2pt5d should be re-compiled.

- The “Effective width of third (i.e. phi) dimension (km)” specified in **simulation-spherical.info** is the spacing between assumed repeating sources, i.e. identical sources are evenly spaced along model azimuth ϕ . This spacing was chosen to be 1200 km in both examples of section 5, large enough to not affect the solution in the areas being analyzed, which are restricted to relatively small ϕ . The computation time of visco2pt5d is inversely proportional to the value of this spacing. It is the user’s judgement (or tests with different spacings could be done) to choose this spacing bearing in mind the tradeoff between accuracy and speed of the computation.
- The cell sizes in the horizontal and vertical dimensions are specified in the “theta-length of each cell (radians)” and “z-length of each cell (km)” array entries in **simulation-spherical.info**. (The theta-length values in radians can be multiplied by the radius of the earth (6371 km) to translate them into horizontal cell sizes in km.) These lengths should be smallest in the near-source region and may be larger at farther distance from the source. The postseismic displacement field at earth’s surface is expected to be of wavelength equal to the elastic layer thickness or greater – the elastic layer thickness in the near-source region and greater at farther distance from the source. The postseismic displacement field at depth generally may be of wavelength equal to the distance of a given observation depth from the base of the elastic layer (depending also how deep the model source extends). In the case that postseismic deformation near the base of the elastic layer is desired, smaller horizontal and vertical cell sizes would be required in the near-source region.
- The “minimum wavelength in third dimension (km)” specified in **simulation-spherical.info** is the minimum wavelength involved with the m-summation in equations 1 and 2. For postseismic deformation at earth’s surface, it should be set to approximately the elastic layer thickness or less (30 km in Examples 1 and 2; 20 km in Example 3).
- The most time-consuming part of the computation is the computation of Laplace-transformed displacements done in the second run of visco2pt5d (out of the total three runs) in the examples. The code has been designed to be run trivially in parallel by telling visco2pt5d in standard input what fraction of the considered Laplace transform parameters are to be done. A variation on ‘example1.x’ – ‘example1-2proc.x’ repeats Example 1 but assigns one-half of the computation to one process and the other half to another process, thereby cutting down the computation time of this step by a factor of 2

(assuming the computer has at least two cores). ‘example1-2proc.x’ will produce identical output to ‘example1.x’.

Appendix A. Evaluation of the Inverse Laplace Transform

Pollitz (2003) proposed a method for an inverse Laplace transform in which the Laplace transform $\tilde{f}(s)$ is represented as a weighted sum of functions $[s(s + s_0\alpha_j)]^{-1}$ over a number of collocation points $\{\alpha_j\}$, plus a term proportional to s^{-1} , i.e.,

$$\tilde{f}(s) = \left(\sum_{i=1}^N C_i \frac{1}{s(s + s_0\alpha_i)} \right) + C_{(N+1)} \frac{1}{s_0 s} \quad (\text{A-1})$$

where s_0 is a reference Laplace transform parameter. In the time domain this yields a superposition of decaying exponentials representing post-seismic motions and a step function that represents a static offset, i.e.,

$$f(t) = L^{-1}[\tilde{f}(s)] = \left(\sum_{i=1}^N \Re(C_i) \frac{1 - \exp[-s_0\alpha_i t]}{s_0\alpha_i} \right) + \Re[C_{(N+1)}] \frac{H(t)}{s_0} \quad (\text{A-2})$$

where $H(t)$ is the Heaviside step function. The weights are determined by sampling $\tilde{f}(s)$ at a set of sample points $\{s_j, j=1, J\}$, i.e., obtaining sample values $\{\tilde{d}(s_j), j=1, J\}$, then defining an inverse problem for the C_i such that eqn A-1 optimally represents $\tilde{d}(s_j)$. Pollitz (2003) employed $N = 7$ collocation points and $J = 12$ sample points in order to represent $\tilde{f}(s)$. That resulted in estimates of $f(t)$ in the time domain very accurate up to $t \sim 150/s_0$.

Pollitz (2003) chose the $\{s_j\}$ through a process of trial and error, based on the ability to replicate test functions, each defined by a decaying expo-

ential with decay time $\geq 1/s_0$. Here we revise the approach to extend the validity up to $t \sim 1000/s_0$, employing a grid search for the $\{s_j\}$ based on minimization of a misfit function in the time domain involving a sum over a set of test functions.

To fit the set of observations $\{\tilde{d}(s_j), j=1, J\}$ with a function $\tilde{f}(s)$ of the form of eqn A-1, we define a cost function

$$C = \sum_{j=1}^J \left| \tilde{d}(s_j) - \tilde{f}(s_j) \right|^2 \quad (\text{A-3})$$

The solution for the $\{C_i\}$ is obtained by minimizing C and can be written in the form

$$C_i = \sum_{j=1}^J \tilde{d}(s_j) \left[\left(\sum_{l=1}^N A_{il}^{-1} \frac{1}{s_j(s_j + s_l)} \right) + A_{i(N+1)}^{-1} \frac{1}{s_js_0} \right] \quad (\text{A-4})$$

where A_{il}^{-1} is the il -component of the inverse of the matrix \mathbf{A} with elements

$$A_{il} = \begin{cases} \sum_{j=1}^J \frac{1}{s_j(s_j + \alpha_i s_0)} \frac{1}{s_j(s_j + \alpha_l s_0)} & i \leq N, l \leq N \\ \sum_{j=1}^J \frac{1}{s_j(s_j + \alpha_i s_0)} \frac{1}{s_js_0} & i \leq N, l = N+1 \\ \sum_{j=1}^J \frac{1}{s_j(s_j + \alpha_l s_0)} \frac{1}{s_js_0} & i = N+1, l \leq N \\ \sum_{j=1}^J \left[\frac{1}{s_js_0} \right]^2 & i = N+1, l = N+1 \end{cases} \quad (\text{A-5})$$

We now employ a set of trial functions $\tilde{d}(s) = \tilde{g}_k(s)$, where

$$\tilde{g}_k(s) = \begin{cases} \frac{1}{s(s + \beta_k s_0)} & k = 1, K \\ \frac{1}{ss_0} & k = K+1 \end{cases} \quad (\text{A-6})$$

Let $C_i^{(k)}$ be the solution of eqn A-4 for the k th trial function, and define the associated reconstruction of the original function as

$$\tilde{f}_k(s) = \left(\sum_{i=1}^N C_i^{(k)} \frac{1}{s(s + s_0\alpha_i)} \right) + C_{(N+1)}^{(k)} \frac{1}{s_0 s} \quad (\text{A-7})$$

With the aim of designing an inverse Laplace transform valid from time 0 to $1000/s_0$, we finally define a misfit function in the time domain

$$M = \sum_{k=1}^K \int_0^{1000/s_0} [f_k(t) - g_k(t)]^2 dt \quad (\text{A-8})$$

In intended applications, s_0 is the reciprocal of the minimum material decay time of the viscoelastic model (which may correspond to a Kelvin element or a Maxwell element of a Burgers body).

The misfit function will depend upon the choices of several sets of parameters, particularly the sample points $\{s_j, j=1, J\}$. Our strategy for designing an optimal inverse Laplace transform is to select fixed sets of collocation points $\{\alpha_j\}$ and decay parameters of the test functions $\{\beta_j\}$ and to vary the values of sample points such that M is minimized. Specifically, we define $N = 11$ and

$$\alpha_1, \dots, \alpha_{11} = 2, 1, \frac{1}{2}, \frac{1}{5}, \frac{1}{10}, \frac{1}{30}, \frac{1}{100}, \frac{1}{300}, \frac{1}{1000}, \frac{1}{3000}, \frac{1}{10000} \quad (\text{A-9})$$

and define $K = 9$ and

$$\beta_1, \dots, \beta_9 = 0.005, 0.01, 0.05, 0.2, 0.3, 0.5, 0.7, 0.85, 1.0 \quad (\text{A-10})$$

With these fixed sets, we determine $J = 28$ sample points through a global search to minimize M using a simulated annealing procedure. This yields the $\{s_j, j=1, 28\}$ and the 12×12 matrix inverse \mathbf{A}^{-1} . In the EXAMPLES-VISCO3D folder, these quantities are contained in the file ‘INVLAPL.PARAM’. Subroutine LAPL (in SOURCE/visco3dsubs.f) then evaluates the inverse Laplace transform using eqns A-2 and A-4.

Figures A-1, A-2, and A-3 show the fit of eqn A-2 to test functions

$$d(t) = [1 - \exp(-t/\tau)] \frac{\tau}{\tau_0} \quad (\text{A-11})$$

for different ratios of τ/τ_0 .

Reference

Pollitz F.F. , 2003. Postseismic relaxation theory on a laterally heterogeneous viscoelastic model, Geophys. J. Int., 155, 57–78.

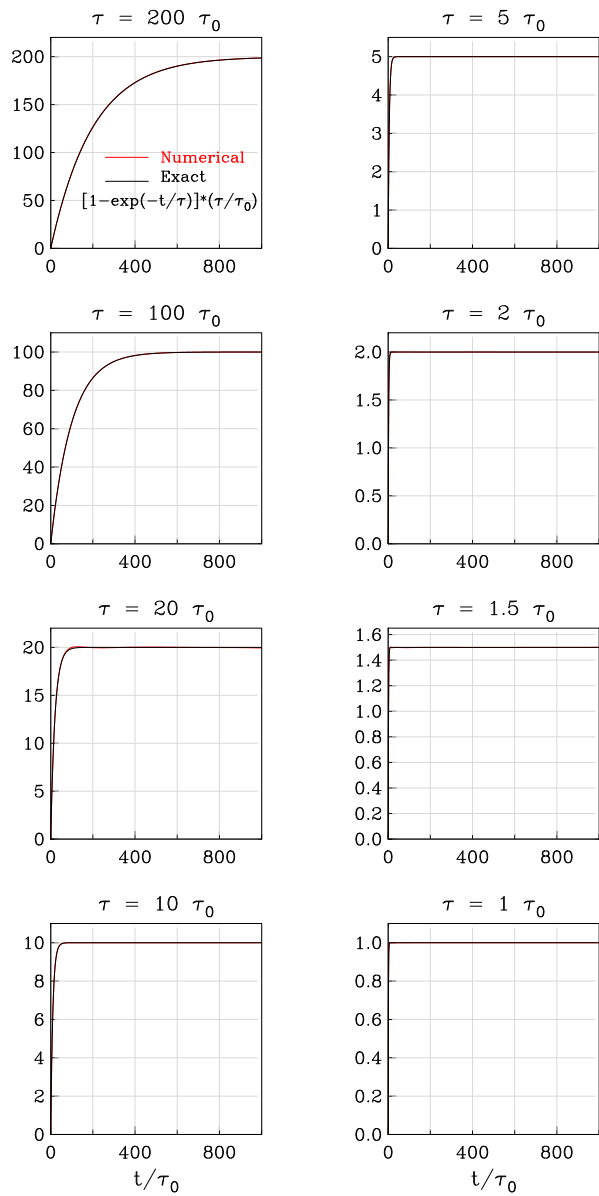


Figure A-1: Fit of eqn A-2 to exponentially-decaying test functions of the form of eqn A-11.

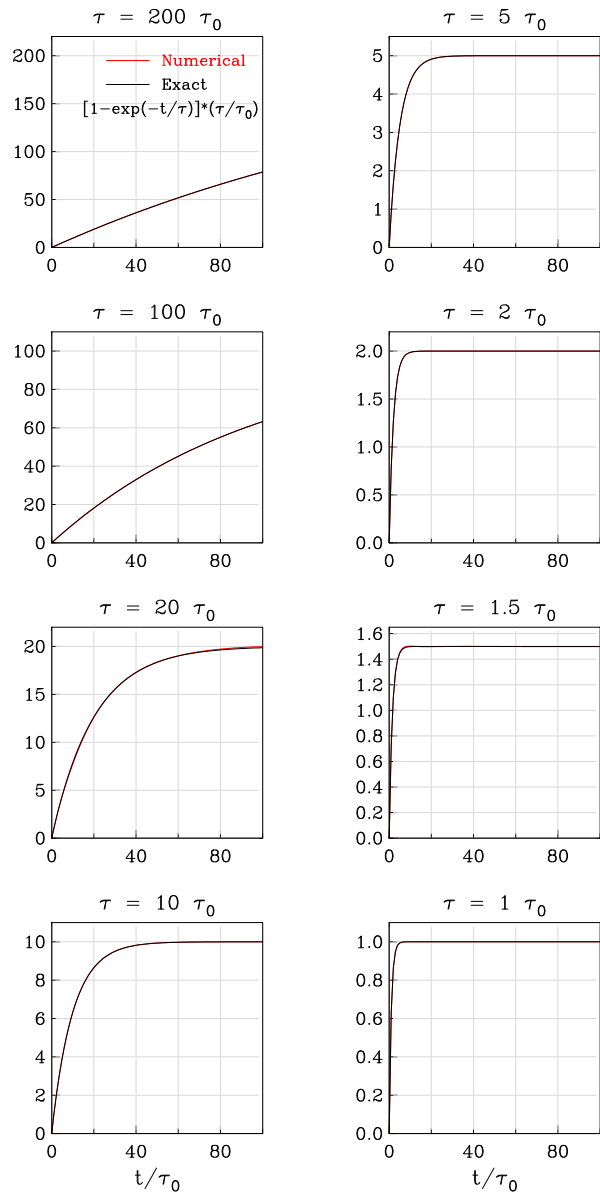


Figure A-2: Same as Figure A-1 with a different scale of the x-axis.

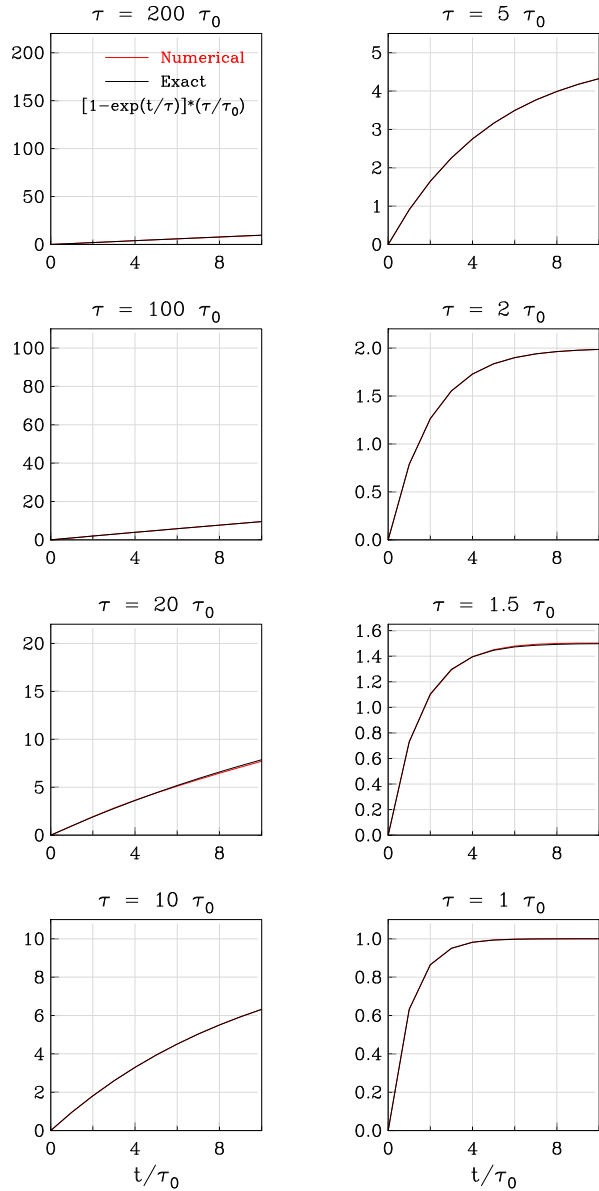


Figure A-3: Same as Figure A-1 with a different scale of the x-axis.